Mining Spatial-temporal Correlation of Sensory Data for Estimating Traffic Volumes on Highways

Yanling Cui[1,2], Beihong Jin[1,2*], Fusang Zhang[1,2], Boyang Han[1,2], Daqing Zhang[3]
1. State Key Laboratory of Computer Sciences, Institute of Software, Chinese Academy of Sciences, China
2. University of Chinese Academy of Sciences, Beijing, China
3. Institute Mines-Telecom, Telecom SudParis, CNRS SAMOVAR, France

ABSTRACT

Sensory data are often of low quality, for example, data are incomplete, ambiguous, or indirect, which has become the bottleneck of many data-driven applications. Two kinds of data which are handled in the paper for estimating traffic volumes on highways are no exception. In particular, the traffic volume data obtained from the loop detectors are accurate but sparse, and the mobile signaling data for estimating relative traffic volumes are wide in coverage and low in cost, but they are indirect and inaccurate. Keeping the characteristics of data in mind, the paper proposes a data fusion approach named Polaris which extends compressive sensing to estimate traffic volumes on highways. The Polaris analyzes the sparsity of the traffic volumes reported by detectors, mines the spatial-temporal correlations between the two kinds of data, and then gives the computational steps in the light of compressive sensing. Experiments are conducted on the large-scale real signaling data and the loop detector data. The experimental results show that the Polaris has the lowest estimation errors in comparison with several other methods. The corresponding Polaris system has been built and deployed in Fujian Province, China. It can obtain real-time traffic volumes on the highways with full coverage at a very low cost. [1]

CCS CONCEPTS

• **Information systems** → Data mining; • **Information systems applications** → Miscellaneous

KEYWORDS

Data Fusion, Compressive Sensing, Spatial-temporal Constraint, Traffic Volume, Intelligent Transportation Systems

MobiQuitous 2017, November 7–10, 2017, Melbourne, VIC, Australia

ACM ISBN 978-1-4503-5368-7/17/11…$15.00
https://doi.org/10.1145/3144457.3144489

1 INTRODUCTION

Traffic volume is an important indicator of real-time traffic conditions on highways. It is expected to be obtained in a full-coverage, high-accuracy, low-cost and real-time way. The real-time traffic volumes can support dynamic traffic navigation, which is convenient for drivers to make travel plans. In the case of traffic accidents and other emergencies, real-time traffic volumes can be used to assist administrators in making decisions on traffic guidance. In addition, the traffic volumes can also be used to calculate carbon emissions, thereby providing data support for environmental monitoring.

With the aid of wireless networks and various sensors, different sensory data can be obtained and used for detecting traffic volumes. However, the low quality inherent in data brings the challenge to obtain the accurate traffic volumes on highways with full coverage in real-time. For example, data from loop detectors are accurate but from specific cross-sectional points, which implies that they only reflect the partial traffic conditions. The complete traffic conditions need to be reconstructed from partial and incomplete data. Moreover, such fixed-device solution suffers from high costs of deployment and maintenance and high failure rates. The GPS data from probe vehicles can also be used to obtain traffic volumes. However, it is more difficult to get accurate volumes, because at present the GPS data only come from particular kinds of vehicles (such as taxis, buses, etc.) and the number of probe vehicles on highways is limited.

According to the traffic theory, the traffic volumes can be derived from the vehicle speeds or densities on the same road segments, as long as the FDs (Fundamental Diagrams, including volume-speed diagram, volume-density diagram and speed-density diagram) are established for each road segment to reflect the inherent relationship between traffic flow parameters. But this indirect method relies on historical traffic data of each road segment, and these historical data may be missing or inaccurate.

We note that mobile phones have become the necessities of daily life. When a mobile phone user moves along with a vehicle, the mobile phone will interact with the base stations near the roads and generates specific signaling records. In particular, on highways, due to the full coverage of base stations and the enclosed nature of highways, the number of trajectories formed by signaling data from mobile phones (hereinafter referred to as signaling volume) can be viewed as an indirect measurement of

traffic volumes. However, estimating traffic volumes with inaccurate and indirect data is far from straightforward.

As an effort to deal with low quality sensory data, in the paper, we fuse two kinds of data to estimate traffic volumes on highways. One is the data of loop detectors on highways, and the other is the mobile phone signaling data from a mobile communication system. Since both kinds of data come from existing systems, no extra devices are needed to be installed. We analyze these two kinds of data, and the analysis results show that the signaling volumes are related to the volumes from detectors (hereinafter referred to as detector volumes). Therefore, we mine the spatial-temporal correlation between these two kinds of data for estimating the traffic volumes of road segments where no loop detectors are installed, and ultimately obtain the overall real-time traffic volumes.

In detail, we firstly propose an adaptation of the edit distance to signaling trajectories to match the signaling trajectories to highways, and then estimate the signaling volumes. Secondly, we construct multiple linear regression (MLR) models by analyzing the relationships between the signaling volumes on different road segments, where these models are employed to describe the spatial correlation between the traffic volumes on different road segments. Finally, taking detector volumes as measurement data, using a Toeplitz-like matrix as the temporal constraint matrix of measurement data and combining the spatial constraint matrix of different road segments, we establish an optimization goal of traffic volume estimation in the light of compressive sensing. We adopt an iterative procedure to solve the optimization equation and then obtain the real-time traffic volumes. The above data fusion approach is named Polaris. Based on the real signaling data and loop detector data, we conduct extensive experiments to compare the Polaris with other three methods, the experimental results show that the Polaris has the lowest errors on traffic volume estimation. With the Polaris at the core, we build a real-time traffic volume monitoring system of the same name, which at present can monitor the traffic volumes on the nine highways in Fujian Province of China.

The remainder of the paper is organized as follows. Section 2 introduces the related work. Section 3 shows some analyses of real-world data, including signaling data and loop detector data. Section 4 gives the problem formulation and the description of the Polaris in detail. Section 5 contains the experimental evaluation. Finally, the paper is concluded in Section 6.

2 RELATED WORK

As a large amount of sensory data are collected, traffic monitoring using sensory data receives much attention from researchers and a variety of approaches are presented. Some approaches rely on data from loop detectors [1, 2], surveillance cameras [3, 23], or GPS devices equipped on vehicles [4]. Some approaches adopt signaling data of mobile phones from mobile communication systems [5, 6]. Some other approaches fuse different sensory data to obtain the traffic conditions [7, 8].

The researches most relevant to this paper are the studies on traffic volumes by exploiting sensory data.

For traffic volume prediction, [9] proposes a latent space model for road networks which considers both topological and temporal properties of road networks. Using the loop detector data as input, the model can estimate the traffic patterns and their evolution over time. The model performs better than existing time series prediction techniques (e.g., ARIMA and SVR). However, the number and the physical meanings of the attributes of vertices in latent spaces are uncertain, which inevitably leads to the weak interpretability of the model. Also for the same goal, [10] uses GPS data of vehicles. By using the historical trajectories of the taxies, the authors obtain the traffic distribution for the edges on the directed graph of a road network and then establish the probabilistic transition matrix for directed edges. They obtain the traffic prediction results at the next moment via multiplying the traffic matrix of the current time by the traffic transition matrix. Unfortunately, the accuracy of this prediction depends on the number of GPS-equipped vehicles.

For traffic volume estimation, [11] uses the GPS data from taxies and urban context information (such as road topology, POI data, weather conditions). By combining with vehicle speed related features from GPS trajectories and urban context features, the authors adopt a Bayesian network model to obtain a high-level feature associated with the traffic volume, which can be used to estimate the traffic volumes on the roads. However, the high-level feature is inferred from the Bayesian network, which is an unsupervised process. No evidences are given to indicate the link between the high-level feature and the actual volume.

With the wide use of the mobile phones, adopting mobile signaling data or CDRs (Call Detail Records) to infer the traffic volume become feasible, where CDRs can be viewed a subset of signaling data. Reference [12] aims at getting the relative volumes of traffic on routes. For this purpose, the authors mine handover patterns from CDRs, and then match these handover patterns to routes. Here, the time-consuming drive tests are needed to obtain the drive duration spent on the cell sectors or SNRs (Signal Noise Ratios) of cell tower antennas. So, the implementation cost is not negligible. Reference [13] builds six models for inferring the traffic volumes on the roads by mining the CDRs. Among the proposed models, the physical model is the most accurate in terms of errors (MAE, MARE, MedARE), and correlations (Spearman rank correlation coefficient, Pearson coefficient) between the estimates and detector values. However, this highest coefficient is still less than 60%. Meanwhile, the physical model makes some assumptions which cannot be satisfied in reality, e.g., the travel distance and time in a cell must be known in advance and stable. Reference [14] exploits handover records in the signaling data to train a multinomial logit model and an artificial neural network model to estimate the traffic volumes where only three coarse-grained categories (i.e., high, medium and low traffic levels) are defined. Their classification accuracy to the three traffic levels is 76.4% and 78.1%, respectively. Similarly, [15] also finds out the relationship between the number of vehicles and handover in cellular network. However, the authors build a multiple linear regression model to capture the relation and the model can reach an R-square statistic of 0.798. We note that the existing methods

of estimating traffic volumes through signaling data cannot avoid the dilemma that the accuracy is not high enough.

Data fusion approaches usually combine static sensory data with roving ones with the expectation of taking advantages of the strengths of different data and avoiding their weaknesses. In [16], the authors collect GPS locations of taxies and the counts from loop detectors installed at some intersections, and build logistic regression models to link the loop count to the number of passing taxies. They develop an algorithm to infer the traffic volumes on the road segments not equipped with loop detectors. In [17], traffic related events are detected by fusing a variety of data sources, including fixed sensors installed at intersections and mobile sensors mounted on public transport vehicles. In order to ensure the accuracy of data, the authors utilize a crowdsourcing component to solve the inconsistency of the sensors. Furthermore, a Gaussian process based method is used to estimate the traffic flow of the road segments covered by sensors.

Different from the previous work, we propose to fuse loop detector data and mobile signaling data for calculating the traffic volumes on highways with full coverage for the first time. Specifically, in order to get traffic volumes of road segments where the loop detectors are not installed, we rely on the above two kinds of data to mine spatial-temporal correlation for traffic volumes. We regularize spatial-temporal constraints to extend the compressive sensing framework, and give the reasonable inference steps for reconstructing the missing data. Our approach relaxes the strict restrictions on the data that are required by the original compressive sensing framework. By this way, our approach can take actual perceived data as input and achieve real-time traffic volume estimation with high accuracy.

3 REAL WORLD DATA ANALYSES

In order to understand the characteristics of the signaling data and loop detector data, we collect the real data generated along the nine highways (i.e., G3, G15, G25, S35, G70, G72, G76, G1501, G1514) in Fujian Province, China. The data include the signaling records from CMCC (China Mobile Communications Corporation) Fujian branch and the loop detector data on the highways in Fujian from Department of Transportation of Fujian Province.

3.1 Spatial-temporal Distribution

On the nine highways whose total length is over 2600 kilometers, 224 loop detectors together with 628 coil sensors are in service. Loop detectors can accurately report the traffic volumes at the locations where they are installed, but the location distribution of loop detectors is uneven. For example, on G1514, the average distance between two loop detectors is about 2.2 kilometers, but on G76 and G70, the corresponding average distances are about 129.5 kilometers and 29.9 kilometers, respectively. For all the nine highways, the average distance between two loop detectors is about 11.9 kilometers. In short, the loop detectors are sparsely distributed.

By comparison, 2017 base stations are deployed along the nine highways in Fujian, and the average distance between two base stations is about 1.32 kilometers. Even for S35 where the deployment of base stations is the sparsest, the average distance between two base stations is only 3.59 kilometers. In general, a signaling record consists of a user identifier (encrypted), a timestamp, a location area code (LAC), a cell ID, a signaling type ID (e.g., 01 for voice, 02 for short message, 03 for data service, 04 for handover out, 05 for handover in, 06 for periodical location update, 07 for power on or off).

We refer to the road between two consecutive ramps on a highway as a road segment. Thus, according to the locations of the ramps, the nine highways are segmented into 383 road segments.

After we specify 15 minutes as a time slice, we calculate the time coverage of two kinds of data within a day. That is, we calculate the ratio of the number of road segments with available signaling/loop detector data to the number of the total road segments every 15 minutes. Meanwhile, we calculate the space coverage of data on the nine highways. That is, for each road segment, we calculate the ratio of the number of time slices with available signaling/loop detector data to the number of the total time slices in a day. Based on these ratios, we plot the CDFs of the time and space coverage.

Fig. 1(a) shows the 3-day CDFs of time coverage on all the nine highways. From Fig. 1(a), as for signaling data, we can find that nearly 96% of time slices have the coverage of more than 94%. This means that almost all road segments have reports in almost all day. As for loop detector data, the time coverage is less than 47%. This indicates that more than 53% of road segments have no reports throughout a day. Fig. 1(b) shows the 3-day CDFs of space coverage on nine highways. For signaling data, we find from Fig. 1(b) that nearly 95% of road segments have coverage of more than 90%. This means that these road segments have reports for more than 90% of a day. And for loop detector data, the space coverage is 0 for 53% of the road segments. These road segments are the ones without loop detectors.

In brief, statistics from the real-world data show that the loop detector data are sparse and the signaling data are dense in space and time. This gives us an idea that is to estimate volumes of the road segments without loop detectors with the help of signaling data.

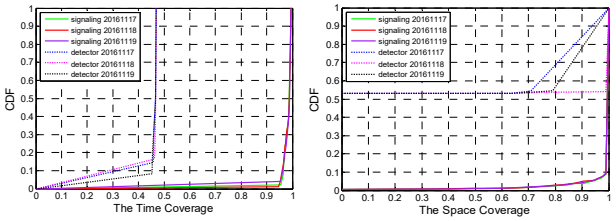

(a) CDFs of the time coverage (b) CDFs of the space coverage

Figure 1: Time and space coverage of signaling data and loop detector data.

3.2 Traffic Volume Correlation

Intuitively, the traffic flows of different road segments are correlated. Our empirical study opens it out.

We collect the volume data from the loop detectors occurred on Fujian highways in the first week of Nov. 2016 and then find that the data cover 180 road segments.

Fig. 2 shows the pair-wise traffic correlation distribution of all 180 road segments, where the correlation is measured by the *Pearson Correlation Coefficient* (PCC) of the two detector volumes occurred at the same time slices but on two road segments. From Fig. 2, we see that about 82% pairs of road segments have relatively strong correlation (i.e., PCC $\geq$ 0.6). This means that multiple road segments are linearly dependent on each other. Those correlations mainly reflect the direct traffic correlations between two road segments. The remaining 18% may contain rich indirect correlation opportunities. To mine the traffic correlations for the traffic estimation, both direct and indirect correlations should be explored and a generic traffic correlation model is desired to capture such relations.

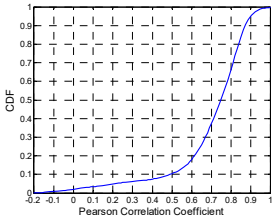

Figure 2: CDFs of pair-wise road segment correlations.

3.3 Relation between Signaling Volumes and Detector Volumes

We can exploit the signaling data to obtain the signaling volumes (see Section 4.5 for more details). However, the signaling volumes are not equal to the real traffic volumes, because there may be more than one person in a vehicle, which is abbreviated to the multi-person scenarios. The method in Section 4.5 does not merge signaling trajectories of multiple persons on a vehicle into one. Therefore, to reveal the relation between detector volumes and signaling volumes at the same time and in the same space, we conduct the following empirical study on a large number of the real-world data.

First, we observe the detector volumes and signaling volumes on a road segment where a loop detector is deployed. Fig. 3 lists the two kinds of volumes on a same road segment of G15 on Nov. 29, 2016. From Fig. 3, we can see that there is a strong linear relation between the two kinds of volumes. We conduct the F-test and t-test on the fitting linear equation. The resulting P-values of F statistics (i.e., significance F) and t statistics are close to 0 (less than 10^{-10}), which show that the linear relation between the two traffic volumes is significant and the effect of the signaling volume on the detector volume is also significant. On the other hand, the resulting adjusted R square is 0.934, which shows the goodness of fit of the linear model is fairly good.

Then, we want to determine whether the linear relations between the two kinds of volumes hold for any road segment. Therefore, we build the regression models for the detector volumes and signaling traffic volumes on each road segment and observe their errors.

Considering the significant periodic patterns of traffic volumes, we organize the days in a week into three categories, i.e. “Each Day of Week”, “Workdays/Non-workdays”, and “All Days together”, where non-workdays contain Saturdays, Sundays and any holidays. Alternatively, we can set the time-of-day category more flexible, varying from 15 minutes to 24 hours at an interval of a multiple of 15 minutes. For example, we can set Workdays/Non-workdays as the day-of-week category and 2 hours as the time-of-day category, which results in $2 \times 12=24$ groups of regression parameters.

Using four-week (i.e., from Nov. 1 to Nov. 28, 2016) data of nine highways, we determine the regression models by the typical cross-validation method, that is, divide the four-week data into 4 one-week testing sets and 4 associated three-week training sets. We train the regression parameters using the training set and apply the parameters to the left-out test set to observe the test errors. Fig. 4 shows training and test RMSE errors of the leave-one-out cross validation after applying the linear regression models for a road segment. As expected, the training errors decrease when we use more complex models; they decrease as the number of time-of-day slots increase. However, the test error does not always decrease as the model complexity increases, which is generally known as over-fitting. Fig. 4 shows that the lowest test error is achieved using All Days with the 15-minute slot, though substantially similar results are achieved by using Workday/Non-Workday with 1-hour as the category of time-of-day.

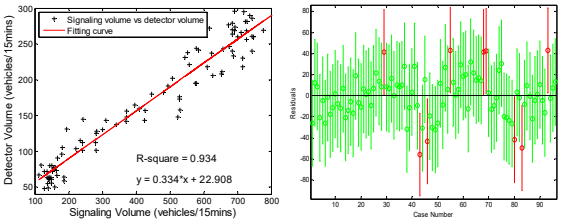

(a) The fitting between the signaling volumes and the detector volumes

(b) The fitting residuals

Figure 3: The signaling volumes and the detector volumes on the 29th road segment of G15 (from Shenyang to Haikou) on Nov. 29, 2016

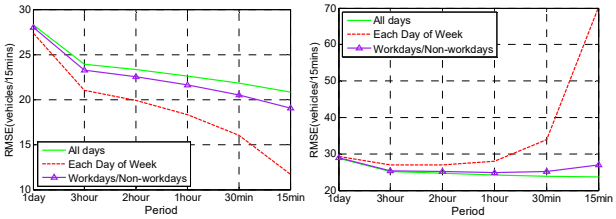

(a) The training errors

(b) The test errors

Figure 4: The training errors and test errors of different regression models

The above regression models and their errors illustrate that even if the multi-person scenarios may take place, the linear relationship exists between the signaling volumes and detector volumes on a same road segment where a loop detector is deployed. Based on this, we believe that the linear relationship should exist on all the road segments, i.e., if the loop detector is deployed on every road segment, there exists the linear relationship between signaling volumes and detector volumes on every road segment. The linear relationship will be not affected by the multi-person scenarios.

These observation results drive us to in Section 4 use the correlation between signaling volumes on road segments to approximately reflect the correlation between traffic volumes on road segments.

4 TRAFFIC VOLUME ESTIMATION

In this section, we formulate the problem of traffic volume estimating first, and then give a detailed description of the Polaris approach. In brief, the Polaris is built upon the basic compressive sensing framework. It converts the traffic volume estimation into an optimization problem under spatial-temporal constraints from traffic flows. Further, it presents a learning algorithm to solve the optimization problem.

4.1 Problem Formulation

For highways with n road segments in total, we use an $m \times n$ nonnegative matrix to describe highway traffic volumes within m time slices. Here, a time slice is set to 15 minutes as default.

Let $X_{m\times n}$ and $\widehat{X}_{m\times n}$ be the real and estimated traffic volume matrix, respectively, the problem of detecting traffic conditions is to find the $\widehat{X}_{m\times n}$ with a minimum $\| X_{m\times n} - \widehat{X}_{m\times n} \|_F$. Here, $\|\cdot\|_F$ is the Frobenius norm of a matrix, i.e., $\|X\|_F \coloneqq \sqrt{\sum_{i,j}(X_{ij})^2}$. More specifically, let $\boldsymbol{x} = [x_1, \cdots, x_n]$ and $\hat{\boldsymbol{x}} = [\hat{x}_1, \cdots, \hat{x}_n]$ be the row which denotes the real and estimated vehicle volumes at the current time slice in $X_{m\times n}$ and $\widehat{X}_{m\times n}$, respectively. The $\hat{\boldsymbol{x}}$ with a minimum $\sqrt{\sum_{k=1}^{n}(x_k - \hat{x}_k)^2}$ are expected. That is, Mean Absolute Error (MAE), Root Mean Square Error (RMSE), and Mean Relative Error (MRE) can be used to measure the closeness between the observation values and real values of the traffic conditions at the same time slice.

Given a signaling stream and a loop detector data stream, we can calculate signaling volumes on the road segments (see Section 4.5), and take detector volumes to form the measurement matrix of traffic volumes, denoted as $M_{m\times n}$. In the matrix $M_{m\times n}$, column j denotes the time series of traffic volumes over the *j-th* road segment and row i denotes the traffic volumes on every road segment at time slice *i*. Due to the sparsity of loop detectors, the matrix $M_{m\times n}$ is not complete where elements of many columns are undefined. However, in the traffic flow scenario, the multiple rows in $M_{m\times n}$ should be linearly dependent on each other, so do the multiple columns. In particular, according to the analytical results in Section 3, the relationship between different columns can be captured by signaling volumes on the road segments.

From these known conditions, we present the Polaris.

4.2 Basic Compressive Sensing Framework

For the traffic volume estimation, we can only obtain some available entries in $X_{m\times n}$, i.e., the available entries in the measurement matrix $M_{m\times n}$. In consideration of the features of traffic volumes, a plausible solution $\widehat{X}_{m\times n}$ is shown in (1).

$$\begin{aligned} &\min rank(\widehat{X}_{m\times n}) \\ &s.t.\ B_{m\times n}.\times \widehat{X}_{m\times n} = M_{m\times n} \end{aligned} \tag{1}$$

where $B_{m\times n}$ is the indication matrix where $B_{m\times n} = [b_{ij}] = \begin{cases} 0, & \textit{if the traffic volume on the } j\textit{-th road} \\ & \textit{segment is unknown at time slice } i \\ 1, & \textit{otherwise} \end{cases}$, $.\times$ is an operator of Hadamard (element wise) product.

Minimizing $rank(\widehat{X}_{m\times n})$ is a non-convex optimization problem and is NP-hard. Therefore, in the light of the compressive sensing method [18], $\widehat{X}_{m\times n}$ can be recovered by transforming (1) to (3) in the following way.

First, since the nuclear norm $\|\cdot\|_*$ of the matrix is the tightest convex envelop for the matrix rank, it is usually adopted to replace the rank. As thus, the non-convex problem in (1) can be converted to the convex problem as shown in (2) [19, 20]. Specifically, if the restricted isometry property holds, minimizing the nuclear norm equals to the rank minimization exactly for a matrix of low rank [21].

$$\begin{aligned} &\min \| \widehat{X}_{m\times n} \|_* \\ &s.t.\ B_{m\times n}.\times \widehat{X}_{m\times n} = M_{m\times n} \end{aligned} \tag{2}$$

where $\| \widehat{X}_{m\times n} \|_* \coloneqq \sum_{i=1}^{rank(\widehat{X}_{m\times n})} \chi_i(\widehat{X}_{m\times n})$, and $\chi_i(\widehat{X}_{m\times n})$ is the *i-th* largest singular value of $\widehat{X}_{m\times n}$.

Secondly, to obtain $\widehat{X}_{m\times n}$ satisfied the (2), we make use of the SVD-like factorization, and let $\widehat{X}_{m\times n} = U\Sigma V^T = LR^T$, where $L = U\Sigma^{1/2}$ is a $m \times r$ matrix, $R = V\Sigma^{1/2}$ is a $n \times r$ matrix. There exist many possible factorization results of $\widehat{X}_{m\times n}$, however, what we need is to find the matrix L and R that minimize the summation of their Frobenius norms, i.e., L and R should satisfy the following (3).

$$\begin{aligned} &\min \| L \|_F^2 + \| R \|_F^2 \\ &s.t.\ B_{m\times n}.\times (LR^T) = M_{m\times n} \end{aligned} \tag{3}$$

Besides, $r \geq rank(X_0)$ should be satisfied as a constraint condition, where X_0 is a solution to (1). If so, then (2) is equivalent to (3) [21].

In practice, L and R that strictly satisfy (3) are likely to lead to an undesirable result due to two reasons. First, a traffic volume matrix usually approximates low-rank but may not be really low in the rank. Second, there is noise in the measurement matrix, and strictly satisfying the constraints may lead to the over-fitting problem. Considering these factors, we convert (3) into a convex optimization in (4) and use the Lagrange multiplier method to solve it.

$$\min \| B_{m\times n}.\times (LR^T) - M_{m\times n} \|_F + \lambda(\| L \|_F^2 + \| R \|_F^2) \tag{4}$$

where the Lagrange multiplier λ controls a tunable tradeoff between rank minimization and accuracy fitness to the measured data. λ is set to 50 as default.

4.3 Spatial-temporal Constraints

Using the resulting L and R from solving (4) to complete $\widehat{X}_{m\times n}$ cannot get the satisfying results, that is, there are still missing values in $\widehat{X}_{m\times n}$. The reason is because in the original $M_{m\times n}$, all the elements of many columns are undefined. To deal with it, the traffic volume features in $X_{m\times n}$ should be mined. As the prior knowledge, we know that the traffic matrix $X_{m\times n}$ has the additional spatial-temporal structure, e.g., the rows or columns of $X_{m\times n}$ close to each other (in some sense) are often close in value. Therefore, we incorporate into (4) the spatial-temporal constraints which the traffic volumes have to abide by, and propose to solve the optimization problem as shown in (5).

$$\begin{aligned} \min \quad & Loss = \| B.\times (LR^T) - M \|_F^2 + \lambda_1 (\| L \|_F^2 + \| R \|_F^2) + \\ & \lambda_2 \| T(LR^T) \|_F^2 + \lambda_3 \| (LR^T) S^T \|_F^2 \end{aligned} \tag{5}$$

where λ_1 controls a tunable tradeoff between rank minimization and accuracy fitness, λ_2 and λ_3 are used to weight the temporal constraints and spatial constraints, respectively. S and T are the spatial and temporal constraint matrices respectively and they express our knowledge about the spatial-temporal structure of the traffic matrix. In the following, we discuss how to choose S and T.

For the traffic volume estimation, the temporal constraint matrix T is supposed to express the temporal smoothness of traffic flows, in other words, the change between two consecutive time slots should be small. Thus, the $Toeplitz(0,1,-1)$ matrix becomes a suitable candidate of the temporal constraint matrix. The $Toeplitz(0,1,-1)$ matrix refers to the matrix in which elements on the main diagonal are given by 1, the elements on the first upper diagonal are given by -1, and the others are given by 0. We choose the first *m-1* rows of an $m \times m$ $Toeplitz(0,1,-1)$ to form the matrix T, i.e.,

$$T = \begin{bmatrix} 1 & -1 & 0 & \cdots & 0 \\ 0 & 1 & -1 & \ddots & \vdots \\ 0 & 0 & 1 & \ddots & 0 \\ \vdots & \vdots & \ddots & \ddots & 0 \\ 0 & 0 & \cdots & 1 & -1 \end{bmatrix}_{m-1\times m} \tag{6}$$

This temporal constraint matrix intuitively expresses the fact that time-adjacent traffic volumes on the same road segment are often similar. By minimizing $\| T(LR^T) \|_F^2$, we seek a minimization of differences between temporally adjacent elements. Since the temporal constraint is an inherent feature of traffic flows, this additional constraint can filter out much noise and more errors in LR^T estimation.

The spatial constraint matrix is used to express which columns of a real traffic volume matrix are close to each other, but due to the arbitrary ordering of columns in the traffic volume matrix, a simple matrix like T is not appropriate.

We find S through Multiple Linear Regression (MLR) models which are built from historical signaling volumes of the road network and express the correlation of traffic volumes among different road segments. More specifically, for each road segment r_i, an MLR model is built for its signaling volume v_{r_i} with respect to the signaling volumes of all other road segments in the road network, as shown in (7).

$$v_{r_i} = \sum_{j=1, j\neq i}^{n} \beta_{r_i, r_j} \times v_{r_j} = \boldsymbol{v}_{r_i}^T \boldsymbol{\beta}_{r_i} \tag{7}$$

where $\boldsymbol{v}_{r_i}$ and $\boldsymbol{\beta}_{r_i}$ are two $(n-1)\times 1$ vectors, and n is the total number of road segments in the road network. The vector $\boldsymbol{v}_{r_i} = [v_{r_1}, \cdots v_{r_{i-1}}, v_{r_{i+1}}, \cdots v_{r_n}]^T$ represents the signaling volumes of the rest *n-1* road segments except r_i. The vector $\boldsymbol{\beta}_{r_i} = [\beta_{r_i, r_1}, \cdots \beta_{r_i, r_{i-1}}, \beta_{r_i, r_{i+1}}, \cdots \beta_{r_i, r_n}]$ records the corresponding coefficients of each road segment. With sufficient training data, we can estimate the regression coefficient vector $\boldsymbol{\beta}_{r_i}$ using the least-square method, which minimizes the formula in (8).

$$\sum_{q=1}^{W} (v_{r_i}^q - \sum_{j=1, j\neq i}^{n} \beta_{r_i, r_j} \times v_{r_j}^q)^2 \tag{8}$$

where W is the total number of time slices in training data set and $v_{r_i}^q$ is the signaling volume of road segment r_i in the *q-th* time slice. As a result, S can be given with the form of (9).

$$S = \begin{bmatrix} -1 & \beta_{r_1, r_2} & \cdots & \beta_{r_1, r_n} \\ \beta_{r_2, r_1} & -1 & \cdots & \beta_{r_2, r_n} \\ \vdots & \vdots & \ddots & \vdots \\ \beta_{r_n, r_1} & \beta_{r_n, r_2} & \cdots & -1 \end{bmatrix}_{n\times n} \tag{9}$$

where the *i-th* row corresponds to the MLR model of road segment r_i if we move v_{r_i} to the right-hand side in (7).

Given historical signaling volumes, we can iteratively train the MLR model in (7) and derive all regression coefficients β_{r_i, r_j} needed by the matrix in (9).

For each road segment r_i, we do not exactly know with which set of road segments it actually correlates before the MLR model is trained. In (7), the signaling volume v_{r_i} is expressed using traffic conditions of all other *n-1* road segments. However, in the real world, a road segment tends to be more correlated with only a certain number, but not all, of road segments. If correlating all road segments to each road segment, the over fitting may occur and huge computation overhead is unnecessarily triggered. Therefore, for any road segment r_i, the traffic correlation would be more reasonably represented by its top-k correlated road segments rather than all other *n-1* road segments. Following this idea, we simplify the model in (7) by pruning the number of unknown coefficients from *n-1* to *k*. Meanwhile, while training the MLR models, merely *k* coefficients are necessary to be learnt. After selecting the top-k correlated road segments, we simply set the rest of coefficients to 0.

In practice, we train the MLR models to construct S with the signaling data three weeks before the current time slice, and update S once a day.

After giving the method of obtaining T and S, we design a learning algorithm to solve (5).

4.4 Learning Algorithm

To derive L and R from (5), we design a learning algorithm in which the alternating least-squares procedure is applied many a time.

Specifically, the learning algorithm includes the following steps. First, L and R are initialized randomly. Next, one of L and R is taken to be fixed and the other to be the optimization variable. Then, the optimization variable is solved as follows.

If letting L be fixed and R be the optimization variable, and letting R^T and M be divided by column, then the Loss function in (5) can be transformed to the following formula.

$$\begin{aligned} Loss = & \sum_{i=1}^{n} \| DiagB(:,i) \times L \times R^T(:,i) - M(:,i) \|_F^2 + \\ & \lambda_1 (\| L \|_F^2 + \| R \|_F^2) + \lambda_2 \| T(LR^T) \|_F^2 + \lambda_3 \| (LR^T) S^T \|_F^2 \end{aligned} \tag{10}$$

where Diag($\boldsymbol{a}$) is a matrix with the elements in vector $\boldsymbol{a}$ as the diagonal elements. Further, we have (11).

$$\begin{aligned} & Loss = \\ & \sum_{i=1}^{n} (R(i,:)L^T DiagB(:,i) - M(:,i)^T) \times (DiagB(:,i) \times L \times R^T(:,i) - M(:,i)) \\ & + \lambda_1 (tr(LL^T) + tr(RR^T)) + \lambda_2 tr(RL^T T^T TLR^T) + \lambda_3 tr(RL^T LR^T S^T S) \\ & = \sum_{i=1}^{n} R(i,:)L^T DiagB(:,i) LR^T(:,i) - 2tr(RL^T M) + tr(M^T M) + \\ & \lambda_1 (tr(LL^T) + tr(RR^T)) + \lambda_2 tr(RL^T T^T TLR^T) + \lambda_3 tr(RL^T LR^T S^T S) \end{aligned} \tag{11}$$

where $tr(A)$ represents the trace of the matrix A.

By letting the derivative of Loss with respect to R be 0, we can obtain (12).

$$\begin{bmatrix} R(1,:)L^T DiagB(:,1)L \\ ... \\ R(i,:)L^T DiagB(:,i)L \\ ... \\ R(n,:)L^T DiagB(:,n)L \end{bmatrix} + R(\lambda_1 + \lambda_2 L^T T^T TL) + \lambda_3 S^T SRL^T L = M^T L \tag{12}$$

Equation (12) has $n \times r$ unknown variables and $n \times r$ equations. By solving (12), R can be obtained.

However, if fixing R and letting L be the optimization variable, then the Loss function can be transformed to the equivalent form as shown in (13).

$$\begin{aligned} Loss = & \| B^T . \times (RL^T) - M^T \|_F^2 + \lambda_1 (\| L \|_F^2 + \| R \|_F^2) + \\ & \lambda_2 \| (RL^T) T^T \|_F^2 + \lambda_3 \| S(RL^T) \|_F^2 \end{aligned} \tag{13}$$

The solving method of (13) is similar to the one of (10).

After getting the value of the optimization variable, we swap the roles of L and R, and continue to apply the alternating least-squares procedure until the obtained L and R are convergent.

4.5 Signaling Volume Estimation

After we receive the signaling records from the interface of the telecommunication system, we discard the signaling data whose locations are not on the highways, filter the signaling data with abnormal movement features (e.g., teleportation), and further identify and get rid of the ping-pong handovers and cell oscillation. Now, we are ready to estimate signaling volume.

Let $\{ B_r \}$ be the base station sequence along the road r. Let $S_u(t_j, b_k)$ be a signaling record that user u connects to base station b_k at the time point t_j, where b_k is given by a (LAC, Cell Id) pair in the signaling record. Thus, the signaling trajectory of user u will be represented by the base station sequence $\{ S_u \}$.

We design an edit distance based method to match a signaling trajectory with road segments. Here, the edit distance is defined as the minimum number of edit operations that converts the $\{ S_u \}$ to $\{ B_r \}$. Considering the characteristics of $\{ B_r \}$ and $\{ S_u \}$, we define the following three edit operations:

1) Delete a base station in $\{ S_u \}$. The operation will be applied when the mobile phone connects a base station that is not included in $\{ B_r \}$, whose rationality is that the user carrying with the phone and moving on the highway may accidentally connect to a base station far away from the road instead of the one in $\{ B_r \}$.

2) Add a base station to $\{ S_u \}$. As we know, when a user is traveling on road r, the mobile phone carried by the user does not necessarily interact with every base station in $\{ B_r \}$ and generate the corresponding signaling records. For such scenarios, we will apply the add operation to $\{ S_u \}$ when the original $\{ S_u \}$ misses some base stations in $\{ B_r \}$.

3) Swap two adjacent base stations in $\{ S_u \}$. Swap operations are necessary, because the order of the base stations in the $\{ S_u \}$ in some scenarios (e.g., communication overload at some base stations) is not necessarily consistent with the one the user has passed through.

Let $B[i]$ and $S[j]$ be the *i-th* base station in $\{ B_r \}$ and *j-th* base station in $\{ S_u \}$, respectively. Let $dist(i, j)$ be the distance between $\{B[1],...,B[i]\}$ and $\{S[1],...,S[j]\}$. We have $dist(0,i) = i$, $dist(j,0) = j$ for $i = 1,2,...,len(B_r)$, and $j = 1,2,...,len(S_u)$. And most of all, we have a state transition function as (14).

$$dist(i,j) = \min \begin{cases} dist(i-1, j) + 1 \\ dist(i, j-1) + 1 \\ dist(i-1, j-1), \quad when B[i] = S[j] \\ dist(i-2, j-2) + 1, \\ \qquad when B[i] = S[j-1] \wedge B[i-1] = S[j] \end{cases} \tag{14}$$

Based on (14), we design the corresponding dynamic programming method to solve the edit distance between $\{ B_r \}$ and $\{ S_u \}$.

In the implementation of the Polaris, we keep the signaling records i.e., $\{ S_u \}$ within the specified duration (e.g., 4 hours) in memory. We check the user trajectories on the roads every t minutes (i.e., a time slice), that is, search the substring $B_r(i, j)$ of $\{ B_r \}$, where i is the location of the first base station in $\{ B_r \}$ that appears in $\{ S_u \}$ and j is the location of the last base station in $\{ B_r \}$ that appears in $\{ S_u \}$. If the condition $j - i \geq \delta_s$ holds, then we consider it is possible for the user u to be the one on the road r. Next, we calculate the edit distance between $\{ S_u \}$ and

$B_r(i, j)$. Then, we select the road segments of the road with the minimum edit distance as the road segments the user u is travelling. Finally, we increment the signaling volumes on the corresponding road segments by 1.

5 EVALUATION

We evaluate our approach from different aspects. First, we compare the traffic volumes estimated by our approach with detector volumes on specific road segments where loop detectors are installed. Then, we give an overall visualization of the traffic volumes and show the correlation between the estimates and the real traffic volumes. At last, we compare our approach with the other three methods.

5.1 Case Study on Specific Road Segments

In the first group of experiments, we randomly select 10% road segments installed with loop detectors as the test set, and treat the detector volumes as the ground truth on these road segments. The rest detector volumes in one week (i.e., from Nov. 22 to Nov. 28, 2016) before the current time slice are taken as the input of the measurement matrix. Signaling volumes of three weeks before the current day are used to construct the spatial constraint matrix S. Fig. 5 shows the comparison between the estimated volumes and the detector volumes of Nov. 29, 2016 on four road segments randomly chosen from the test set. We can see that the estimated volume (X-axis) is strongly linearly correlated with the real volume (Y-axis). The fitting line is close to the line function of y=x, which demonstrates the high estimation accuracy.

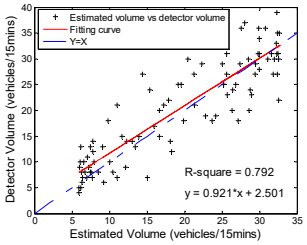

(a) 6th road segment of Fujian section of G3, from Taipei to Beijing

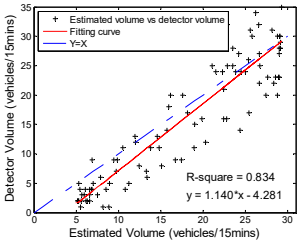

(b) 4th road segment of Fujian section of G25, from Changchun to Shenzhen

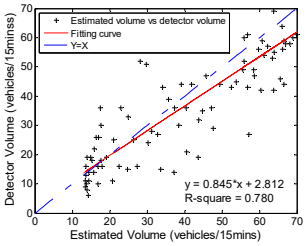

(c) 54th road segment of Fujian section of G15, from Shenyang to Haikou

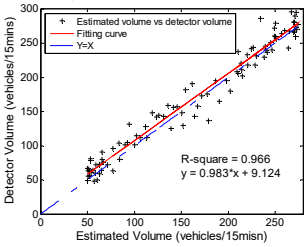

(d) 29th road segment of Fujian section of G15, from Shenyang to Haikou

Figure 5: The estimated volumes vs. the real volumes on four road segments

5.2 Overall Visualization and Correlation

Fig. 6 gives the visualization of traffic volumes on nine highways in the Fujian Province. From Fig. 6(a), we can see that there is much traffic on G15 from 8:45 to 9:00 on Nov. 29, 2016. This is because the G15 crosses the coastal cities which have booming transportation demands than inland cities, resulting in the relatively busy traffic. Fig. 6(b) shows the GUI of our developed traffic volume monitoring system (Polaris). The lines of different colors represent the different highways, and the different line width represents the different traffic volumes. If the user clicks on a road segment, the corresponding volume is annotated on it.

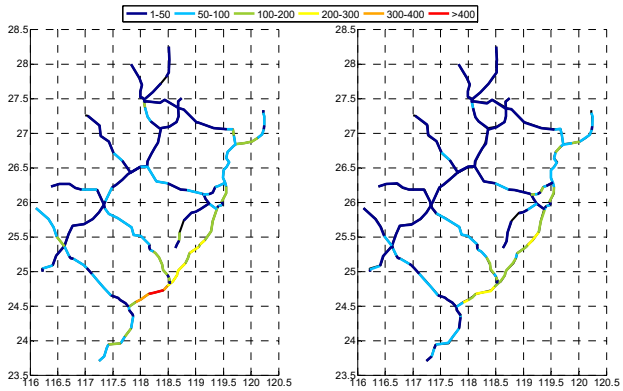

(a) The visualization of bidirectional traffic volumes for nine highways in Fujian Province from 8:45 to 9:00 on Nov. 29, 2016

(b) Polaris: Traffic volume monitoring system

Figure 6. The visualization of traffic volumes

In the second group of experiments, for all the road segments in the test set, we calculate the estimated volumes on Nov. 29, 2016, and then plot the CDF of the Pearson correlation coefficients between the estimated volumes and corresponding detector volumes. The results are shown in Fig. 7. From Fig. 7, we can see that the estimated volumes and detector volumes on 95.2% of the road segments appear strong correlations, i.e., the correlation coefficient is higher than 0.6. Especially, the two volumes on 71.4% of the road segments appear extremely strong correlations, i.e., the correlation coefficient is higher than 0.8, which indicates that the Polaris provides the overall estimation with high confidence.

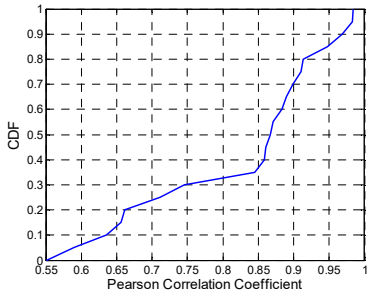

Figure 7: The CDF of the Pearson correlation coefficients between the estimated volumes and corresponding detector volumes on Nov. 29, 2016

5.3 Estimation Errors of Different Methods

We conduct a comparative experiment, comparing our method with other three methods: linear regression method, high order singular value decomposition (HOSVD) based method [22], and weighted average method [16]. The methods chosen for comparison are briefly described as follows.

Linear regression method: By setting Workdays/Non-workdays as the day-of-week category and 1 hour as the time-of-day category, using the two traffic volumes three weeks before the current time slice as input, we train the linear model for each road segment where a loop detector is installed. As for the road segments without any loop detector, the models of adjacent road segments are employed. When the signaling stream arrives, we use the above linear models to estimate volumes.

HOSVD based method [22]: Taking the results of the linear regression method as input, we construct a tensor of size $383\times7\times24\times4$. Here, 383 is the number of road segments, 7 is the number of days in one week, 24 is the number of hours in a day, 4 is the number of time slices in an hour. We use the historical traffic volumes of one week before the current time slice as input. Then, HOSVD is applied to decompose the tensor. In our experiment, the half components of each dimension are considered the principal components. So, the first half components are used to reconstruct the tensor. The reconstructed tensor is thought to be the estimated results.

Weighted average method [16]: First, the similarity between road segment i and j is quantified by:

$$s(i,j)=\frac{1}{d(i,j)}\times\frac{1}{a(i,j)}\times\frac{1}{l(i,j)}\times\frac{1}{t(i,j)} \tag{15}$$

where $d(i,j)$ is the Euclidean distance between road segment i and road segment j, $a(i,j)$ is the angular difference between the orientation of road segment i and that of road segment j, $l(i,j)$ is the difference between number of lanes of road segment i and that of road segment j, $t(i,j)$ is the difference between signaling volume for road segment i and that of road segment j. Next, the traffic volume for road segment i without any loop detector is estimated as follows.

$$v_t(i)\times\sum_{j\in O}w_i(j)\frac{v(j)}{v_t(j)} \tag{16}$$

where $v_t(i)$ is the signaling volume for road segment i, $v(j)$ is the detector volume for road segment j where a loop detector is installed, O is the set of all road segments with loop detectors, $w_i(j)$ is the normalized similarity of road segment j for road segment i, which is calculated as follows.

$$w_i(j)=\frac{s(i,j)}{\sum_{k\in O}s(i,k)},\quad \forall j\in O \tag{17}$$

We choose the data that span a duration of one week prior to the current time to form the measurement matrix. We randomly remove some percentage of road segments with loop detectors and regard the detector volumes on these road segments as the ground truth. The removal ratio ranges from 10% to 90% at an interval of 10%. If the removal ratio is 0, i.e., the data is complete, then it is unnecessary to be interpolated. If the removal ratio is raised to 100%, then no method can work.

Using the data on Nov. 29, 2016 as an input stream, we execute the above four methods to estimate the traffic volumes on all the road segments in real time, i.e., the traffic volumes are estimated every 15 minutes. We choose the traffic volumes at the locations of removal loop detectors and compare them with the detector volumes. We take MAE, RMSE, MRE as metrics to evaluate the accuracy of the traffic volumes.

Fig. 8 shows the performance of the four methods in terms of estimation errors. We can see that our approach outperforms the other three methods under all metrics. When the removal ratio is 10%, the MAE and RMSE is 15.66 and 25.82 per 15 minutes, respectively. The MRE of our method is 38.59%, 41.77% and 112.79% lower than the linear regression method, HOSVD based method and weighted average method, respectively. Our approach fills the missing traffic volumes by capturing spatial and temporal characteristics learned from signaling volumes. As we fully utilize the inherent features of sensory data, the estimated results are better than other methods.

Weighted average method (see the light blue line with right y-axis in Fig. 8) performs the worst. It is because that in [16], the data used to estimate the traffic volumes of road segments without loop detectors are GPS data from taxis. However, we implement the method using signaling data. These two kinds of data have different generation frequency, which decays the estimation accuracy. Especially, when the removal ratio is 90%, the results are extremely bad. From these observations, we find the weighted average method cannot deal with the sparse data perfectly.

The performance of linear regression method is not as good as our approach. The reason behind it is that the regression models of road segments without loop detectors are from adjacent road segments. This is not quite appropriate due to the difference between different road segments, even if there exits the linear relation between the signaling volumes and detector volumes on the same road segment. The performance of the HOSVD based method is close to linear regression method. This is because that the HOSVD based method takes the results of the linear regression method as input. The HOSVD based method can capture the principle components from data and remove the noise.

But if the input data are not with the high fidelity, the HOSVD based method still cannot reconstruct high quality data.

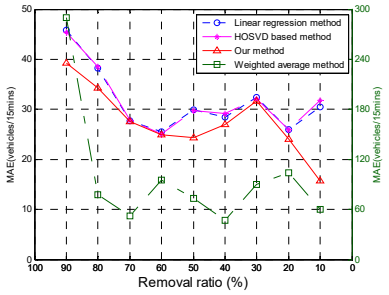

(a) MAEs under different methods

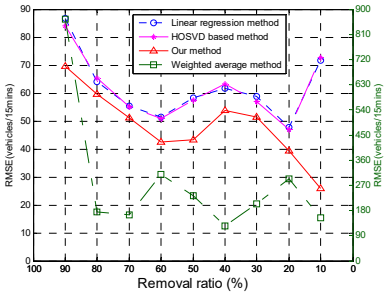

(b) RMSEs under different methods

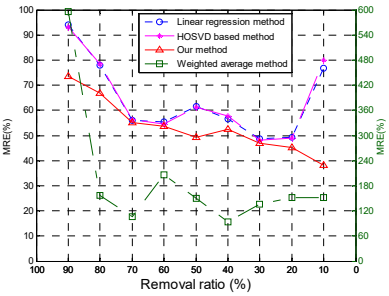

(c) MREs under different methods

Figure 8: Errors under different methods using data on Nov. 29, 2016 as input.

6 CONCLUSION

To our knowledge, we are the first to fuse the loop detector data and signaling data to estimate the traffic volumes on highways. We mine the relations of the two kinds of data themselves and between them, and propose the Polaris for calculating the traffic volumes on highways with full coverage. The resulting traffic volumes not only retain the accuracy of the detector volumes, but also have the characteristics of wide coverage of signaling data. The Polaris extends the basic compressive sensing framework, and the ideas inside the Polaris also offer a practical guidance on mining and utilizing the low-quality data. We conduct extensive experiments to evaluate the Polaris. Compared with other three methods, the Polaris can effectively reduce the errors of traffic volume estimation and satisfy the requirements of practical applications.

ACKNOWLEDGMENTS

This work was supported by the National Natural Science Foundation of China under Grant No. 61472408 and the Ministry of Transportation of China under Grant No. 2015315Q16080.

REFERENCES

[1] J. Kwon, P. Varaiya, and A. Skabardonis. Estimation of Truck Traffic Volume from Single Loop Detectors with Lane-To-Lane Speed Correlation. Transportation Research Record: Journal of the Transportation Research Board, vol. 1856, pp. 106–117, 2003.

[2] D. Wilkie, J. Sewall, and M. Lin. Flow Reconstruction for Data Driven Traffic Animation. ACM Transactions on Graphics, 2013, 32(4): 89:1–89:10.

[3] X. Zhan, R. Li, and S. V. Ukkusuri. Lane-Based Real-Time Queue Length Estimation Using License Plate Recognition Data. Transportation Research Part C: Emerging Technologies, vol. 57, pp. 85–102, 2015.

[4] Zhidan Liu, Zhenjiang Li, Mo Li, et al. Mining Road Network Correlation for Traffic Estimation via Compressive Sensing. IEEE Transactions on Intelligent Transportation Systems, 2016, 17(7): 1880-1893.

[5] Lv M, Chen L, Wu X and Chen G. A Road Congestion Detection System Using Undedicated Mobile Phones, IEEE Transactions on Intelligent Transportation Systems, 2015, 16(6):3060-3072

[6] Janecek A, Valerio D, Hummel K A, Ricciato F, and Hlavacs H. The Cellular Network as a Sensor: From Mobile Phone Data to Real-Time Road Traffic Monitoring. IEEE Transactions on Intelligent Transportation Systems, 2015, 16(5): 2551-2572.

[7] Calabrese F., Colonna M.,. Lovisolo P, Parata D., and Ratti C., Real-Time Urban Monitoring Using Cell Phones: A Case Study in Rome, IEEE Transactions on Intelligent Transportation Systems, 2011, 12(1):141-151.

[8] Beihong Jin, Yanling Cui, Fushang Zhang. Fusing Static and Roving Sensor Data for Detecting Highway Traffic Conditions in Real Time. IEEE International Conference on Computers, Software and Applications, June 10-14, 2016, pp. 807-816, Atlanta, Georgia, USA.

[9] Dingxiong Deng, Cyrus Shahabi, Ugur Demiryurek, Linhong Zhu, Rose Yu, Yan Liu. Latent Space Model for Road Networks to Predict Time-Varying Traffic. ACM International Conference on Knowledge Discovery and Data Mining, 2016:1525-1534.

[10] Pablo Samuel Castro, Daqing Zhang, and Shijian Li. Urban Traffic Modelling and Prediction using Large Scale Taxi GPS Traces. Pervasive Computing. Springer Berlin Heidelberg, 2012:57-72.

[11] Xianyuan Zhan, Yu Zheng, Xiuwen Yi, Satish V. Ukkusuri. Citywide Traffic Volume Estimation Using Trajectory Data. IEEE Transactions on Knowledge and Data Engineering 2017.

[12] Becker R A, Caceres R, Hanson K, et al. Route Classification Using Cellular Handoff Patterns. International Conference on Ubiquitous Computing, 2011: 123-132.

[13] CaceresN, RomeroL M, BenitezF G, etal. Traffic Flow Estimation Models Using Cllular Phone Data. IEEE Transactions on Intelligent Transportation Systems, 2012, 13(3): 1430-1441.

[14] Demissie M G, Bento C. Intelligent Road Traffic Status Detection System Through Cellular Networks Handover Information: An Exploratory Study. Transportation Research Part C: Emerging Technologies, 2013, 32(4):76–88.

[15] Demissie M, Correia G, Bento C. Traffic Volume Estimation through Cellular Networks Handover Information. World Conference on Transportation Research. 2013.

[16] Aslam J., Lim S., Pan X., and Rus D.. City-Scale Traffic Estimation from A Roving Sensor Network. ACM Conference on Embedded Network Sensor Systems, 2012, 141–154.

[17] Artikis A, Weidlich M, Schnitzler F, et al. Heterogeneous Stream Processing and Crowdsourcing for Urban Traffic Management. International Conference on Extending Database Technology. 2014:712-723.

[18] E.J. Candés, T. Tao. The Power of Convex Relaxation: Near-Optimal Matrix Completion. IEEE Transactions on Information Theory. 2010, 56(5):2053-2080.

[19] F.R. Bach. Consistency of Trace Norm Minimization. Journal of Machine Learning Research. 2007, 9(2):2008.

[20] M. Fazel. Matrix Rank Minimization with Applications. Ph.D. dissertation, Department of electrical engineering, Stanford University, California, 2002.

[21] B. Recht, M. Fazel, P.A. Parrilo. Guaranteed Minimum-Rank Solutions of Linear Matrix Equations Via Nuclear Norm Minimization. Siam Review. 2010, 52(3):471-501.

[22] Zhang F, Yuan N J, Wilkie D, et al. Sensing the Pulse of Urban Refueling Behavior: A Perspective from Taxi Mobility. ACM Transactions on Intelligent Systems and Technology, 2015, 6(3):37.

[23] Hajimolahoseini, H., R. Amirfattahi, and H. Soltanian-Zadeh. Robust vehicle tracking algorithm for nighttime videos captured by fixed cameras in highly reflective environments. IET Computer Vision, 2014, 8(6): 535-544